MOVING PROPAGATION OF SUSPICIOUS MYOCARDIAL INFARCTION FROM DELAYED ENHANCED CARDIAC IMAGING TO CINE MRI USING HYBRID IMAGE REGISTRATION

Yixun Liu[1,2,3], *Hui Xue*[1], *Christoph Guetter*[1], *Marie-Pierre Jolly*[1], *Nikos Chrisochoides*[3] *and Jens Guehring* [1]

[1] Siemens Corporate Research, Imaging and Visualization, Princeton, NJ, USA
[2] Department of Computer Science, The College of William and Mary, Williamsburg, VA, USA
[3] Department of Computer Science, Old Dominion University, Norfolk, VA, USA

ABSTRACT

Cardiac magnetic resonance imaging has proved its effectiveness to determine the patient-specific myocardial motion/functional information via the cine imaging and to detect myocardial infarction in the delayed enhanced MRI (DE-MRI). Standard cardiac MR protocols usually acquire these two sets of images across multiple acquisitions with varying imaging slice geometry, pixel spacing and different breath-holdings, which could make the joint inspection of myocardial motion and infarction difficult. The purpose of this work is therefore to develop dedicated post-processing algorithms to register DE-MRI to corresponding cine image and propagate suspicious infarction to all cardiac phases. Suspicious infarction regions delineated in the DE-MRI can be used to define the region-of-interest for the quantification of regional wall motion abnormality. The proposed approaches are applied to 6 patients and the evaluation shows the feasibility of a joint DE-MRI and cine assessment which can yield clinically valuable outcomes.

Index Terms— Image registration, Cardiac magnetic resonance imaging, Delayed Enhanced MRI, Moving propagation

1. INTRODUCTION

Cardiac magnetic resonance imaging has proved its effectiveness to determine the patient-specific myocardial motion/functional information via the cine imaging as well as detection of myocardial infarction appearing hyperintense in the DE-MRI. Recent studies compared myocardial tissue viability revealed in the DE-MRI to the functional deficits measured with cine MRI [1], showing the so-called "peri-infarction zone" defined in DE-MRI is correlated well with the dysfunctional myocardial region defined in cine. This information is potentially valuable for reperfusion therapy, as regional motion of infarction zone defined before the therapy is assessed to evaluate the recovery of myocardium.

THIS WORK IS SUPPORTED IN PART BY NSF GRANTS: CCF-0916526, CCF-0833081, AND CSI-719929 AND BY THE JOHN SIMON GUGGENHEIM FOUNDATION.

Although the clinical value of joint DE-MRI and cine image assessment is exhibited, standard clinical cardiac MR protocols usually acquire two sets of images across multiple measurements with variant imaging plane prescription and multiple breath-holdings. Misalignment and local deformation often appear between cine and DE-MRI, even imaging plane remains unchanged for two acquisitions by careful prescription, mainly due to inconsistent cardiac phases used for acquiring cine and DE-MRI, imperfect cardiac gating and respiratory motion. It is more problematic for patients with arrhythmias as unstable cardiac cycles make it unreliable to identify the matching cine frame acquired in the same cardiac cycle as the DE-MRI.

Without an accurate mapping of infarction zone to cine images, regional myocardial changes in motion pattern caused by suspicious scars could only be visually assessed. The accurate alignment and deformation correction between cine and DE-MRI is thus a necessity for the successful joint assessment, where one aim is to propagate the infarction to all other cine frames throughout whole cardiac cycle and enable the quantitative regional motion pattern analysis.

There are little research focusing on aligning cardiac MR images acquired across acquisitions with different pulse-sequences, compared to the large amount of studies conducted myocardial motion correction within one acquisition. One approach performing joint analysis is to manually segment images from multiple acquisions and the resulting AHA model is matched [2]. Others rely on aligning epicardial surfaces which are delineated before analysis [3]. More recently, a 2D-3D rigid image registration method was proposed to align DE-MRI and perfusion slices to the 3D whole heart coronary angiography volume [4], which enables the visualization of infarction in the 3D context.

The contribution of this work is to develop dedicated post-processing algorithms for aligning DE-MRI with corresponding cine image and propagating suspicious infarction zone to all other cardiac phases. Infarction regions delineated in the DE-MRI can be used to define the region-of-interest (ROI) for the quantification of regional abnormality of myocardial motion. To achieve these goals, we propose to align DE-MRI to

cine image using a hybrid registration algorithm unifying both intensity and feature points into one cost function. Intensity term is used to match two images on a coarse level, playing a role of regularization and dominating the alignment of normal myocardium, while feature point term is robust against contrast changes between DE-MRI and cine as in the latter infarction zone bearing little contrast compared to normal myocardium is largely invisible. The propagation of infarction zone throughout the cine is achieved by estimating myocardial deformation in the cine series using a variational non-rigid registration algorithm with inverse consistent constraint.

2. METHOD

To align the DE-MRI to cine and propagate suspicious infarction, two types of deformation need to be estimated. The first corrects the mis-alignment between DE-MRI and cine and the second quantifies myocardial motion within cine series. Fig. 1 illustrates the proposed procedure.

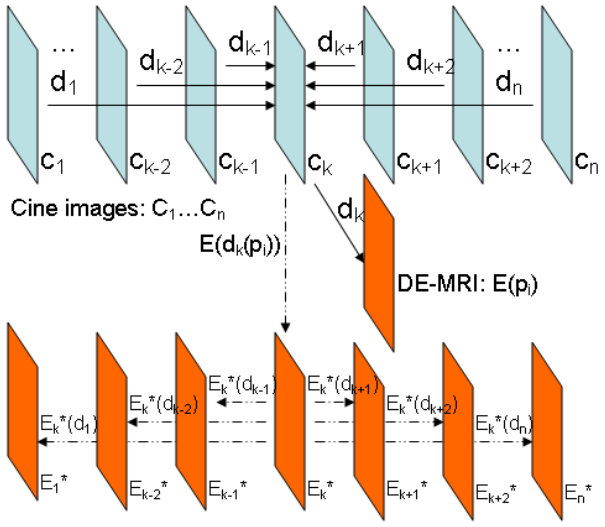

Fig. 1. c_k: the reference frame. d_k: deformation from c_k to the DE-MRI. $d_l, l = 1 \dots n, l \neq k$: deformation from c_l to c_k. Solid line arrow points to the deformation direction and dash line arrow points to the propagation direction. p_i is the position of the pixel with index i.

As multiple cine images are required to cover the whole cardiac phase while one DE-MRI image is usually acquired at a specific temporal phase, the cine image, which is most similar with the DE-MRI, is selected as the reference to which the DE-MRI is registered. Assume the k-th phase is the reference image. The deformation d_k, from c_k to the DE-MRI $E(p_i)$, is recovered by the hybrid registration method and both forward and inverse deformation fields $d_l, l = 1 \dots n, l \neq k$ are recovered by variational method. Once all deformation fields $d_l, l = 1 \dots n$ are computed, the DE-MRI and infarction can be propagated.

2.1. Select the reference frame in the cine

The cine frame, which is most similar with the DE-MRI, is selected as the reference. If available in the database, the trigger time is used to match the DE-MRI. For cine series where trigger time is not recorded, the Cross-Correlation (CC) is computed between every cine image and DE-MRI. The frame with largest CC value is picked.

2.2. Compute deformation fields within cine series

To propagate the suspicious infarction from the reference to all other cine frames, the deformation between cine images is estimated using a fast variational non-rigid registration algorithm [5]. This approach can be considered as an extension of the classic optical flow method. In this framework, a dense deformation field is estimated as the solution to a calculus of variation problem, which is solved by performing a compositional update step corresponding to a transport equation. The regularization is added by low-pass filtering the gradient images which are in turn used as velocity field to drive the transport equation. To speedup the convergence and avoid local minima, a multi-scale image pyramid is created. We selected the local cross correlation as the image similarity measure, as its explicit derivative can be more efficiently calculated than mutual information and still general enough to cope with intensity fluctuation and imaging noise between two adjacent perfusion frames.

Registration of time series such as MR cine is usually performed by selecting a reference phase to which all other phases are registered. This approach is not sufficient as both DE-MRI images and infarction zone which is represented as a contoured region are propagated throughout the cardiac phases. Specifically, deformation fields pointing to the reference phase are required to warp the DE-MRI image while the inverse deformations pointing from reference phase to other frames are needed to warp the infarction contours. We thus extend the above-mentioned registration algorithm to estimate the inverse consistent deformation fields.

A deformation field Φ_{pq} is inverse consistent if $\Phi_{pq} \cdot \Phi_{pq}^{-1} = I$ and $\Phi_{pq}^{-1} = \Phi_{qp}$. Φ_{pq} is retrieved by minimizing the inverse consistent similarity metric:

$$J_{icCC} = J_{CC}(f_p, f_q, \Phi_{pq}) + J_{CC}(f_q, f_p, \Phi_{qp}) \qquad (1)$$

Here J_{CC} is the local cross correlation. f_q and f_p are two cine phases. Their deformation is $\Phi_{pq} : \Re^2 \rightarrow \Re^2$.

We have developed an efficient update scheme of the iterative gradient descent, in order to minimize the inverse consistent similarity in reasonable time [6]. In essence, each deformation field is alternately updated during descending the gradient of similarity measure resulting in an accurate computation of the inverse deformation and a quasi-symmetric registration algorithm. The extra computational effort for inverse consistent deformable registration is only about 10%-15% when compared to Hermosillo et al. [7]. The achieved

inverse consistency not only allows for propagating both images and contours between any two cardiac phases, but also often leads to more accurate quasi-symmetric image registration.

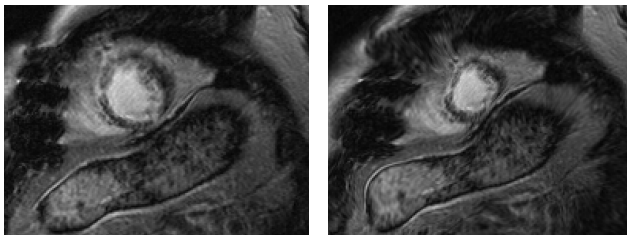

(a) Before registration (b) After registration

Fig. 2. A DE-MRI image is registered to the selected cine frame using the variational registration. The warped DE-MRI shows unrealistic deformation due to enhanced infarction bearing no contrast in cine.

The variational deformable registration method is robust for cine images, as each adjacent image pair shows similar image content and contrast. Unfortunately, it is less suitable to register DE-MRI to cine reference phase, as the former often presents strongly enhanced infarction zone which bears no contrast in the cine series. As a result, the pixel-wise variational registration tends to generate unrealistic large deformation which degrades the image quality of warped DE-MRI images even with aggressive regularization, as demonstrated in Fig. 2.

2.3. Register DE-MRI to the reference cine

To cope with inconsistent visibility or occlusion of infarction zone between DE-MRI and cine and produce robust registration, we propose a hybrid registration algorithm, which unifies intensity-based and point-based similarity into one cost function. This cost function contains two terms: feature point matching term and intensity matching term. Specifically, point matching term is robust against contrast changes and occlusions between DE-MRI and cine. Intensity term enforces the alignment of myocardium with normal contrast uptake, playing a role of global regularization. The underlying deformation is modeled as a Free-from deformation [8], which is a piece-wise cubic polynomial. Compared to pixel-wise variational registration, Free-form deformation is more robust against image content changes.

Free-form deformation (FFD) FFD can be manipulated by a regular control grid with spacing $s_x \times s_y$ for 2D image. FFD is computationally efficient, because the deformation at any point is only influenced by its surrounding 4×4 control points.

For a point p with coordinate (x, y), assume its 4×4 control points are p_{ij}. $i, j = 0, \ldots, 3$. Denote d_{ij} as the displacement vector associated with the control point p_{ij} , the interpolation at point p is defined as,

$$T(p|d_{ij}) = \sum_{i=0}^{3}\sum_{j=0}^{3} B_i(u)B_j(v)d_{ij}, \tag{2}$$

where $u = x/s_x - \lfloor x/s_x \rfloor$, $v = y/s_y - \lfloor y/s_y \rfloor$. B_i is the i-th basis function of B-splines [8].

Cost function Given reference image $R(p_i), i = 1 \ldots N$ and its feature point set $\{s_j\}_{j=1}^{M}$, and floating image $F(p_i)$ and its feature point set $\{t_j\}_{j=1}^{M}$, we define the following minimization problem:

$$\hat{D} = \underset{D}{\operatorname{argmin}}\Big(\frac{\lambda}{M}\sum_{M}\|T(s_j|D) - t_j\|^2 - \frac{\sum_N (R(p_i) - \bar{R})(F(T(p_i|D)) - \bar{F})}{\sqrt{\sum_N (R(p_i) - \bar{R})^2 \sum_N (F(T(p_i|D)) - \bar{F})^2}}\Big) \tag{3}$$

where the first term is point matching and the second term is intensity matching. R is reference image and F is floating image. $\bar{R}$ and $\bar{F}$ are the mean intensity of R and F respectively. D is the unknown parameter set $\{d_{ij}\}$. λ is used to balance the influences of both terms. The value of λ depends on the metric in the intensity term. We experimentally select Cross-Correlation (CC) as the intensity metric and λ is set to be 0.5. The equation 3 is solved by L-BFGS optimization, which is more efficient, compared to simple gradient descent, for high dimensional optimization problems [9].

2.4. Propagate the DE-MRI

Once all deformation fields $d_l, l = 1 \ldots n$ are computed the DE-MRI E can be propagated to yield all n cardiac phases: $E_l^*, l = 1 \ldots n$. First, the DE-MRI E is deformed to E_k^* using $E_k^* = E(d_k(p_i))$. Then E_k^* is propagated to the remaining $n-1$ phases using $E_l^* = E_k^*(d_l(p_i)), l = 1 \ldots n, l \neq k$. Note the propagation of delineated infarction contours requires the inverse deformation fields pointing from reference to other $n - 1$ phases. It is provided by the inverse consistent registration of cine series. To better present propagated DE-MRI, three propagation schemes as shown in Fig. 3 are implemented: whole image propagation, contour propagation and ROI propagation. Whole image propagation resamples the whole DE-MRI to the cine coordinates. Contour propagation

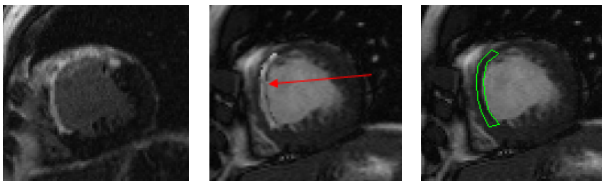

(a) Whole (b) ROI (c) Contour

Fig. 3. Three propagation schemes.

only deforms the scar boundary. ROI scheme transforms the scar region and superimposes it directly on cine images.

3. RESULTS

Both TrueFISP cine and inversion recovery TurboFlash delayed enhancement imaging were performed on 6 patients with suspicious myocardial infarction using the clinical standard protocols. DE-MRI was acquired between 10 and 30 minutes after administering contrast agent. Experiments were conducted using 1.5T Siemens Avanto scanner. For every subject, the slice prescription between cine and DE-MRI acquisitions was kept unchanged to minimize the through-plane displacement. The proposed analysis workflow was applied

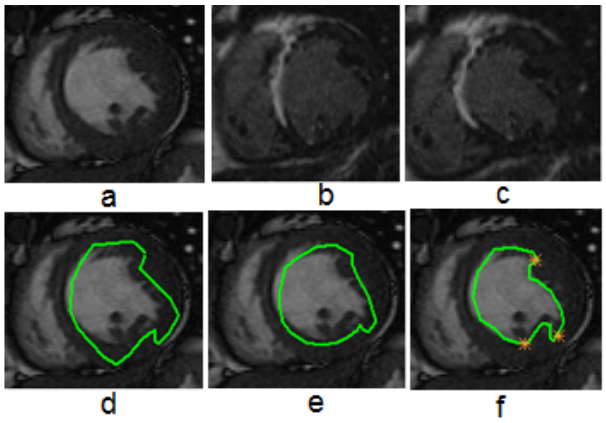

Fig. 4. Comparison between intensity-based method and the hybrid method. a: cine image. b: DE-MRI. c: aligned DE-MRI by CCPD. d: before registration. e: CC registration. f: CCPD registration.

to all datasets and outputs were first inspected. For all cases the hybrid registration produces better alignment. As an illustration of typical performance, Fig. 4 shows a comparison between intensity based registration (Cross-Correlation, CC) and hybrid method (Cross-Correlation with Point Distance, CCPD). We delineate a contour on the aligned DE-MRI by CC registration and a contour on the aligned DE-MRI by CCPD registration. The delineated contour is superimposed on the cine image to show the registration result.

Table 1. Quantitative measures of DE-MRI to cine registration.

	Cine–Original DE-MRI	Cine–CC moco	Cine–CCPD moco
Dice ratio	0.65 ± 0.06	0.64 ± 0.16	0.80 ± 0.08
False positive	0.32 ± 0.08	0.30 ± 0.15	0.14 ± 0.08
False negative	0.39 ± 0.08	0.42 ± 0.18	0.26 ± 0.08
MBE (in mm)	3.40 ± 2.56	3.33 ± 2.75	2.12 ± 1.57

The quantitative evaluation was performed by manually delineating the myocardium on the cine reference frame and aligned DE-MRI image. Four statistical measures are computed to give a comprehensive quantification: Dice ratio (the myocardium overlap ratio); false positive (the percentage area of myocardium labeled in cine but not labeled in DE-MRI); false negative(the percentage area of myocardium not labeled in cine but labeled in DE-MRI); MBE (the myocardium boundary errors, defined as the minimal distances between myocardium contours (endo and epi) extracted from the cine and DE-MRI slices). Table 1 summarizes the results, showing superior performance of hybrid approach. For these 6 datasets, in plane resolution is $1.18 \sim 1.36\ mm^2$. Compared with doing nothing, CC method shows worse performance (lower Dice ratio and higher False negative), demonstrating its characteristic susceptible to the contrast change.

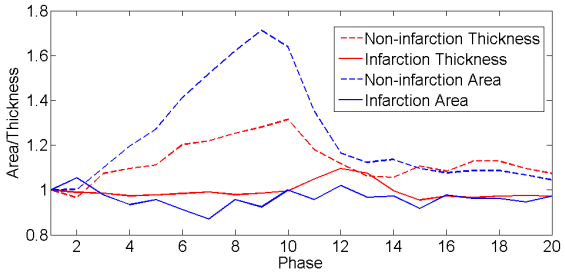

Fig. 5. Area and thickness of both infarction and healthy myocardium over one cardiac cycle.

Fig. 6 shows the propagated DE-MRI and the infarction contours. Suspicious infarction can degrade myocardial contraction. To highlight the potential of the proposed workflow for abnormal motion pattern detection, we delineated the scar region in the DE-MRI and label the myocardial segment containing the scar. Both the contour and segment are propagated to all cardiac phases using the estimated forward/inverse deformation fields. At each phase p, the area of the infarction zone A_p is computed by counting the number of the internal pixels. The thickness T_p is computed by calculating the epi/endo distance of the segment. To alleviate the inter-subject variability, A_p and T_p are normalized with respect to phase 0, i.e., $A_p = A_p/A_0$, $T_p = T_p/T_0$. For the comparison, the normal myocardium is also delineated, of which the area and thickness were computed. Fig. 5 shows the changes of the area and the thickness cross one cardiac cycle for one test case. The area and thickness of healthy myocardium is found to change more significantly over cardiac phases compared to infarction zone.

Table 2. Area/Thickness change %. ACI: Area Change of Infarction zone. ACN: Area Change of Normal myocardium. TCI: Thickness Change of Infarction zone. TCN: Thickness Change of Normal myocardium.

Cases	1	2	3	4	5	6
ACI	4.5 ± 0.1	4.5 ± 0.2	8.4 ± 0.4	9.7 ± 1.1	3.1 ± 0.1	6.3 ± 0.2
ACN	13.1 ± 0.7	4.6 ± 0.2	6.7 ± 0.3	2.5 ± 0.0	10.6 ± 1.1	8.0 ± 0.2
TCI	2.7 ± 0.1	3.8 ± 0.1	5.9 ± 0.3	7.2 ± 0.3	3.7 ± 0.1	5.3 ± 0.2
TCN	23.5 ± 5.1	19.9 ± 4.9	15.5 ± 2.6	7.6 ± 0.7	20.0 ± 3.1	14.6 ± 1.1

To quantify the change potentially caused by the suspicious infarction, we use $(A_p - A_0)/A_0$ to represent the relative area change and $(T_p - T_0)/T_0$, basically the segment

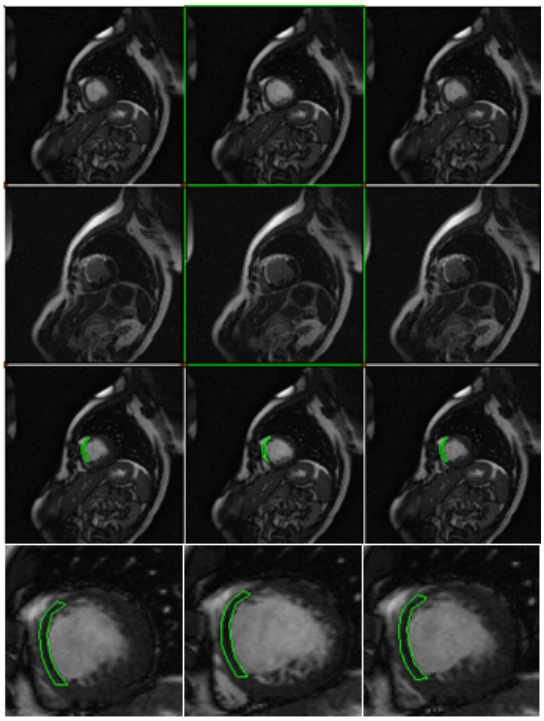

Fig. 6. The first row is the cine images; the second row is propagated DE-MRI and the third row is propagated contour superimposed on the cine. The propagated contours are zoomed in at last row. The image with green box in the first row corresponds with C_k in Fig.1 and the image with green box in the second row corresponds with E_k^*. Due to space limit, we only present the results at three different phases.

strain ratio, to represent the relative thickness change. The mean and variance of 6 cases are listed in Table 2. Case 1 and 5 shows noticeable decrease of both area and thickness changes for the infraction, while thickness dropped more in case 2, 3 and 6. Interestingly, case 4 shows the contrary that relative area change increases for the infarction, although the registration and propagation performed well which was verified by visual reading. While it is known that contrast enhancement of the myocardium is not a specific sign for myocardial infarction [10], we are reluctant to draw any physiological conclusions here. On the other hand, these initial experiments do reveal the feasibility of joint DE-MRI and cine assessment which could lead to more thorough clinical study of regional wall motion changes related to ischemic heart diseases.

4. CONCLUSION AND FUTURE WORK

This paper presents dedicated post-processing algorithms to align DE-MRI images to cine series and propagate the suspicious infarction zone to all cardiac phases. These warped infarctions define the ROI for the quantification of regional abnormality of myocardial motion, which enables the joint cine and DE-MRI assessment. Key algorithmic steps include aligning DE-MRI image to cine using a hybrid registration algorithm combining both intensity and point-based similarity terms. The myocardium deformation within the cine series is recovered by the inverse-consistent non-rigid registration which enables the propagation of both delayed enhancement images and delineated scar regions. Initial experiments show the effectiveness of proposed method and highlight its potentials to perform quantitative motion pattern analysis. We are now proceeding to further validate these methods and apply them to the study of myocardial motion abnormality associated with proved or suspicious ischemic heart diseases.

5. REFERENCES

[1] Miller Stephan, Helber Uwe, Brechtel Klaus, Nägele Thomas, Hahn Ulrich, Kramer Ulrich, Hoffmeister Hans, and Claussen Claus, "Mr imaging at rest early after myocardial infarction: detection of preserved function in regions with evidence for ischemic injury and non-transmural myocardial infarction," *European Radiology*, vol. 13, pp. 498–506, 2003.

[2] M. Breeuwer, I. Paetsch, E. Nagel, R. Muthupillai, S. Flamm, S. Plein, and J. Ridgway, "The detection of normal, ischemic and infarcted myocardial tissue using mri," *International Congress Series*, vol. 1256, pp. 1153 – 1158, 2003.

[3] Setser R.M., O'Donnell T.P., Smedira N.G., Sabik J.F., Halliburton S.S., Stillman A.E., and White R.D., "Coregistered MR Imaging Myocardial Viability Maps and Multi–Detector Row CT Coronary Angiography Displays for Surgical Revascularization Planning: Initial Experience1," *Radiology*, vol. 237, no. 2, pp. 465–473, 2005.

[4] Hennemuth A, Seeger A, Friman O, Miller S, Klumpp B, Oeltze S, and Peitgen HO., "A comprehensive approach to the analysis of contrast enhanced cardiac mr images," *IEEE Trans Med Imaging*, vol. 27, no. 11, pp. 1592 – 610, 2008.

[5] Chefd'hotel C., Hermosillo G., and Faugeras O., "Flows of diffeomorphisms for multimodal image registration," in *IEEE International Symposium on Biomedical Imaging*, 2002, pp. 753–756.

[6] Marie-Pierre Jolly, Christoph Guetter, and Jens Guehring, "Cardiac segmentation in mr cine data using inverse consistent deformable registration," in *IEEE International Symposium on Biomedical Imaging*, 2010, pp. 484–487.

[7] Hermosillo G., Chefd'Hotel C., and Faugeras O., "Variational methods for multimodal image matching," *International Journal of Computer Vision*, vol. 50, no. 3, pp. 329–343, 2002.

[8] Lee S., Wolberg G., and Shin S.Y., "Scattered data interpolation with multilevel B-splines," *IEEE Transactions on Visualization and Computer Graphics*, vol. 3, no. 3, pp. 228–244, 2002.

[9] J. Nocedal and S.J. Wright, *Numerical optimization*, Springer Verlag, 1999.

[10] Bogaert Jan, Goldstein Marcelo, Tannouri Fadi, Golzarian Jafar, and Dymarkowski Steven, "Late Myocardial Enhancement in Hypertrophic Cardiomyopathy with Contrast-Enhanced MR Imaging," *Am. J. Roentgenol.*, vol. 180, no. 4, pp. 981–985, 2003.